PHYSICAL REVIEW A VOLUME 35, NUMBER 12 JUNE 15, 1987

Computational study of radiative transitions in molecular collisions induced by short laser pulses

Hai-Woong Lee
Department of Physics, Oakland University, Rochester, Michigan 48063

Thomas F. George
Departments of Chemistry and Physics & Astronomy, 239 Fronczak Hall, State University of New York at Buffalo, Buffalo, New York 14260

(Received 20 January 1987)

A theoretical study of radiative transitions in molecular collisions occurring in the presence of short laser pulses is carried out within the semiclassical two-state formalism. Transition probabilities are calculated by numerically integrating the Bloch equation for two model systems and the Na-Ar system. At high laser intensities where a short pulse is more effective in inducing transitions than cw radiation, the transition probability exhibits nonlinear character with respect to the pulse intensity. At such high intensities, noncollisional atomic transitions may also be present, which need to be eliminated for an observation of collisional transitions.

I. INTRODUCTION

Atomic and molecular collisions taking place in the presence of laser radiation have been studied extensively in the past.[1] It is now well established both theoretically[2] and experimentally[3] that the presence of strong laser radiation can greatly alter the outcome of collision processes. This is significant as it offers a means of controlling physical and chemical processes by varying laser parameters such as intensity and wavelength. We have suggested in the past that the details of laser radiation (linewidth, temporal variation of the intensity, etc.) need to be carefully examined before the effect of the radiation is accurately determined.[4,5] In particular, we showed that the temporal width of radiation can have a significant effect on electronic transitions occurring via curve crossing: If laser radiation consists of pulses whose duration is shorter than the collision time, transition probabilities may be significantly higher than for the case of cw radiation or long pulses.[5] An experimental study of this short-pulse effect in the Na-Ar system has recently been reported by Sizer and Raymer.[6]

The basic idea behind the short-pulse effect is a closing of transition channels during one half of the collision. It can be best illustrated with the Landau-Zener model,[7] as we described in our earlier paper.[5] If one considers a dipole transition taking place in the presence of cw laser radiation (or a long pulse) of constant intensity I, the Landau-Zener probability is given by

$$P_{\rm cw}=2\exp(-\beta I)[1-\exp(-\beta I)]\ , \tag{1}$$

where β is a constant depending on the details of the system. If, however, the laser radiation consists of a short pulse which illuminates the system on the way in (out) only, the transition at the crossing point on the way out (in) is effectively turned off, and the probability becomes

$$P_s=1-\exp(-\beta I)\ . \tag{2}$$

If the laser intensity is sufficiently high ($\beta I \gg 1$), P_s is significantly higher than $P_{\rm cw}$, indicating that a short pulse can be much more effective in inducing transition than cw radiation or a long pulse.

While the above argument serves to illustrate the basic idea, it does not reveal many complications and difficulties that accompany the detailed theoretical analysis and experimental observation of short-pulse-induced collisions. We note in particular that the short-pulse effect manifests itself strongly at relatively high intensities at which transitions exhibit nonlinear characters. The short-pulse probability P_s cannot stay high at all high values of the intensity because of the Rabi oscillation. If one introduces the concept of the pulse area here, P_s is high only if the pulse area is in the neighborhood of an odd multiple of π. This restricts the range of intensity over which the short-pulse effect is significant, while the Landau-Zener model only requires the intensity to be sufficiently high ($\beta I \gg 1$). Another difficulty arises from the fact that, in order to observe the short-pulse effect, the pulse duration must be shorter than the collision time. With the typical collision time of 10^{-11}–10^{-12} sec, one needs picosecond or subpicosecond pulses. Such ultrashort pulses have large linewidths which may leave channels other than the one under consideration open, especially at high pulse intensities. In particular, noncollisional atomic transitions may occur at asymptotic separations if the laser frequency is not sufficiently far away from atomic resonance. In addition, there are complications arising from different collision partners having different impact parameters and different relative velocities, which require appropriate averaging processes. Effects due to the shape of the pulse, the polarization of the pulse, etc., should also be carefully considered.

It is therefore clear that a quantitatively accurate description of atomic and molecular collisions occurring in the presence of short laser pulses requires a more accurate treatment than the simple Landau-Zener model, especially at high laser intensities. One might adopt, for example, an approach that employs numerical integration of the classical path equation,[8] or, equivalently, of the Bloch equation.[9] This numerical Bloch approach was used by Sizer and Raymer[6] to analyze their experimental data.

At the present time it is not possible to construct a complete theoretical description of the complex collision process occurring in the presence of a short laser pulse. This paper represents an attempt to provide the first step toward such a description. Since the short-pulse effect is important at high pulse intensities, we give special consideration to high intensity effects such as effects due to the Rabi oscillation and noncollisional atomic transitions. We recall that, for a clean observation of the short-pulse effect, one wants to choose a system which exhibits minimal complications arising from such high intensity effects. In order to cover a variety of possibilities, we choose to study two model systems and the Na-Ar system which show different degrees of high intensity effects. Both the Landau-Zener model and the numerical Bloch approach are used to calculate transition probabilities. It is of course the numerical Bloch approach that gives a more accurate description. The Landau-Zener calculations are presented to demonstrate and analyze the limitations of the model.

In Sec. II we give a description of the Landau-Zener model and the numerical Bloch approach. We then describe in Sec. III the two model systems and the Na-Ar system for which our calculations are made. The results of our calculations are presented in Sec. IV, and in Sec. V a discussion is given.

II. THE LANDAU-ZENER MODEL AND THE NUMERICAL BLOCH APPROACH

In this section we describe the two approaches used in our calculations: the Landau-Zener model and the numerical Bloch approach. The former provides a rough estimate of transition probabilities, while for more accurate results we perform numerical integration of the Bloch equation.

The transition we consider is an electric dipole transition induced by collision that occurs in the presence of laser radiation. We assume that the system is prepared in the ground state u_1 before collision and are interested in the transition to an excited state u_2 with absorption of a photon from the laser field. Within the semiclassical two-state formalism,[10] the Schrödinger equation yields the following coupled equations for the probability amplitudes $a_1(t)$ and $a_2(t)$ for the two states u_1 and u_2:

$$i\hbar\frac{da_1(t)}{dt}=W_1a_1+W_{12}a_2 , \tag{3a}$$

$$i\hbar\frac{da_2(t)}{dt}=W_{21}a_1+W_2a_2 , \tag{3b}$$

with the initial condition given by

$$|a_1(0)|=1, \quad a_2(0)=0 . \tag{4}$$

Here the matrix elements $W_i=\langle u_i|H|u_i\rangle$ and $W_{ij}=\langle u_i|H|u_j\rangle$ of the Hamiltonian H vary with internuclear distance and thus with time. The diagonal elements W_1 and W_2 represent the potential-energy surfaces of the two states being considered, and the off-diagonal element W_{12} is given by

$$W_{12}=\langle u_1|-e\mathbf{r}\cdot\mathbf{E}|u_2\rangle=-\boldsymbol{\mu}\cdot\mathbf{E}_0\cos(\omega t) , \tag{5}$$

where $\boldsymbol{\mu}$ is the transition moment ($\boldsymbol{\mu}=\langle u_1|e\mathbf{r}|u_2\rangle$), which in general varies with the internuclear distance, $\mathbf{E}_0$ is the electric field amplitude [$\mathbf{E}=\mathbf{E}_0\cos(\omega t)$], and ω represents the angular frequency of the laser field.

Equations (3) can be transformed to a form in which the Landau-Zener model can readily be applied by the substitution

$$a_1=c_1\exp(in\omega t), \quad a_2=c_2\exp[i(n-1)\omega t] , \tag{6}$$

where n is the number of photons in the laser field before collision. Equations (3) then become

$$i\hbar\frac{dc_1(t)}{dt}=H_{11}c_1+H_{12}c_2 , \tag{7a}$$

$$i\hbar\frac{dc_2(t)}{dt}=H_{21}c_1+H_{22}c_2 , \tag{7b}$$

where

$$H_{11}=W_1+n\hbar\omega, \quad H_{22}=W_2+(n-1)\hbar\omega \tag{8a}$$

and

$$H_{12}=-\boldsymbol{\mu}\cdot\mathbf{E}_0/2 . \tag{8b}$$

In deriving Eqs. (7) we also have made the rotating-wave approximation. The factor $\frac{1}{2}$ appearing in Eq. (8b) is the result of this approximation. Let us assume that the laser field is in resonance with the two states u_1 and u_2 at a certain internuclear distance $R=R_c$, i.e.,

$$H_{22}(R_c)-H_{11}(R_c)=0 . \tag{9}$$

The Landau-Zener probability as the system passes through the crossing point R_c is given by

$$P=1-\exp(-p) , \tag{10a}$$

where

$$p=2\pi[H_{12}(R_c)]^2/\hbar v\gamma\left[1-\left[\frac{b}{R_c}\right]^2\right]^{1/2} , \tag{10b}$$

b is the impact parameter, $\gamma=[d(H_{22}-H_{11})/dR]_{R=R_c}$, and v is the relative velocity of the colliding partners at the crossing point R_c. If the collision occurs in the presence of a short pulse so that the system is illuminated on the way in or out only, the transition probability is given by $P_s=P$. On the other hand, if the system is illuminated both on the way in and out as is the case for cw radiation or a long pulse, the transition probability is given by $P_{\rm cw}=2P(1-P)$.

A more accurate evaluation of the transition probability can be obtained if Eqs. (3) are numerically integrated. It

is, however, more convenient to transform Eqs. (3) to the Bloch form before performing integration. For this purpose we first let $\rho_{ij}=a_i a_j^*$ to obtain

$$\frac{d\rho_{11}}{dt}=\frac{i}{\hbar}H_{12}\rho_{21}+\frac{i}{\hbar}H_{21}\rho_{12}\ , \tag{11a}$$

$$\frac{d\rho_{22}}{dt}=-\frac{i}{\hbar}H_{21}\rho_{12}+\frac{i}{\hbar}H_{12}\rho_{21}\ , \tag{11b}$$

$$\frac{d\rho_{12}}{dt}=\frac{i}{\hbar}(H_{22}-H_{11})\rho_{12}-\frac{i}{\hbar}H_{12}\rho_{22}+\frac{i}{\hbar}H_{12}\rho_{11}\ , \tag{11c}$$

$$\frac{d\rho_{21}}{dt}=-\frac{i}{\hbar}(H_{22}-H_{11})\rho_{21}-\frac{i}{\hbar}H_{21}\rho_{22}+\frac{i}{\hbar}H_{21}\rho_{11}\ . \tag{11d}$$

We now define R_1, R_2, and R_3 as

$$R_1=\rho_{21}\exp(i\omega t)+\rho_{12}\exp(-i\omega t)\ , \tag{12a}$$

$$R_2=i\rho_{21}\exp(i\omega t)-i\rho_{12}\exp(-i\omega t)\ , \tag{12b}$$

$$R_3=\rho_{22}-\rho_{11}\ . \tag{12c}$$

Equations (11) can then be written for R_1, R_2, and R_3 as

$$\frac{dR_1}{dt}=-(H_{22}-H_{11})R_2/\hbar\ , \tag{13a}$$

$$\frac{dR_2}{dt}=(H_{22}-H_{11})R_1/\hbar-2H_{12}R_3/\hbar\ , \tag{13b}$$

$$\frac{dR_3}{dt}=2H_{12}R_2/\hbar\ , \tag{13c}$$

where the rotating-wave approximation has been made, and H_{ij} are defined by Eqs. (8). Equations (13) can be written in vector form as[9]

$$\frac{d\mathbf{R}}{dt}=\mathbf{R}\times\boldsymbol{\eta}\ , \tag{14a}$$

where

$$\boldsymbol{\eta}=-\frac{2H_{12}}{\hbar}\hat{\mathbf{e}}_1-\frac{(H_{22}-H_{11})}{\hbar}\hat{\mathbf{e}}_3\ . \tag{14b}$$

The $\mathbf{R}$ vector precesses clockwise about the effective field $\boldsymbol{\eta}$ with the frequency $|\boldsymbol{\eta}|$. Thus, Eqs. (14) provide a pictorial representation of the transition: As the system approaches the crossing point R_c, $|H_{22}-H_{11}|$ decreases and the rotation axis of the vector $\mathbf{R}$ approaches the x axis. At the crossing point, $\mathbf{R}$ precesses about the x axis, producing a rapid change in R_3, which indicates that the transition is taking place. As the system moves away from the crossing point, $|H_{22}-H_{11}|$ increases and the rotation axis turns from the x axis toward the z axis. At asymptotic separations ($|H_{22}-H_{11}|\gg|2H_{12}|$), the $\mathbf{R}$ vector precesses about the z axis, producing no change in R_3, and thus no transition.

Equations (14) [or Eqs. (13)] are the Bloch equations which are to be integrated subject to the initial condition given by Eq. (4), or, in terms of R_1, R_2, and R_3, by

$$R_1(0)=R_2(0)=0,\quad R_3(0)=-1\ . \tag{15}$$

The main difficulty in integrating these equations arises from the fact that H_{ij} vary with internuclear distance and thus with time in a complicated manner. The time variation of H_{ij} is determined by the collision dynamics, which in turn depends on the potential-energy surfaces of the system. For our calculations, we assume a simple straight-line constant-velocity ($=v$) trajectory, which allows us to obtain the time dependence of H_{ij} directly from its dependence on the internuclear distance. Once the time dependence of H_{ij} is determined, the integration can be performed using the standard fourth-order predictor-corrector method with the Runge-Kutta method as a starter. The accuracy of integration can be checked any time during integration, due to the identity

$$R_1^2(t)+R_2^2(t)+R_3^2(t)=1\ . \tag{16}$$

For the models we consider, the transition occurs mainly in the neighborhood of the crossing point R_c unless the laser intensity is extremely high. If collision occurs in the presence of a short pulse which illuminates the system on the way in or out only, the integration is performed only once through the crossing point to determine the short-pulse probability P_s. To determine the magnitude of the short-pulse effect, this probability P_s must be compared with the cw (or long-pulse) probability $P_{\rm cw}$. If the two crossing points are well separated so that the Stückelberg interference[11] can be neglected, the probability $P_{\rm cw}$ is given by $P_{\rm cw}=2P_s(1-P_s)$.

III. THE SYSTEMS

For our study of the short-pulse effect, we choose to consider two model systems as well as the Na-Ar system for which experimental data exist.[6] Here we give a brief description of each system. Throughout the section we use atomic units unless stated otherwise.

A. Model 1

The first model system is defined by the following equations:

$$H_{22}-H_{11}=0.001\sinh[2(R-R_c)]\ , \tag{17a}$$

$$H_{12}=-\boldsymbol{\mu}_0\cdot\mathbf{E}_0/2\ , \tag{17b}$$

where we take $R_c=9.5$ and $\mu_0=|\boldsymbol{\mu}|=3$. Since this model is characterized by a rapid increase in energy detuning $|H_{22}-H_{11}|$ as R moves away from the crossing point R_c, the transition is highly localized around R_c and the Rabi oscillation is expected to occur only at extremely high intensities. The Landau-Zener model should therefore work well for this model. Also, the energy detuning is large at asymptotic separations, so noncollisional atomic transitions do not occur. This model therefore is expected to exhibit the short-pulse effect most clearly without complications arising from the Rabi oscillation or any noncollisional atomic transition. We also note that the magnitude of the transition momentum $\boldsymbol{\mu}$ is assumed constant (independent of the internuclear distance R), $|\boldsymbol{\mu}|=\mu_0$. This is a good approximation if the transition considered is, for example, the $X\,^2\Sigma-A\,^2\Pi$ transition of Na-Ar.

B. Model 2

The second model system is characterized by the potential-energy surfaces given as

$$W_2 = 3.2\exp(-0.737R) + 0.0744 , \tag{18a}$$

$$W_1 = 0.2\exp(-0.737R) . \tag{18b}$$

These potential-energy surfaces are plotted in Fig. 1. The wavelength of the laser is assumed to be $\lambda = 16\,916$ cm^{-1} (same as the wavelength used by Sizer and Raymer), i.e., $\hbar\omega = 0.0771$. We therefore obtain

$$H_{22} - H_{11} = 3\exp(-0.737R) - 0.0027 . \tag{19a}$$

We also assume

$$H_{12} = -\boldsymbol{\mu}_0 \cdot \mathbf{E}_0/2 , \tag{19b}$$

with $\mu_0 = 3$, as in model 1. From Eq. (19a) we obtain the crossing point to be $R_c = 9.5$. As R moves away from R_c, $|H_{22} - H_{11}|$ increases less rapidly for this model than for model 1, indicating that the transition occurs over a wider range of internuclear distances for this model. Thus the Landau-Zener model is probably less accurate for model 2, especially when the laser intensity is high. The Rabi flopping can also occur more easily since the energy detuning stays low over a relatively long period of time. Another point to note is that the energy detuning $|H_{22} - H_{11}|$ at large R is 0.0027, to which the interaction energy $\mu_0 E_0/2$ becomes comparable at a laser intensity of $\sim 10^{11}$–10^{12} W/cm^2. Thus, the contribution from the noncollisional atomic transition should also be considered for this model.

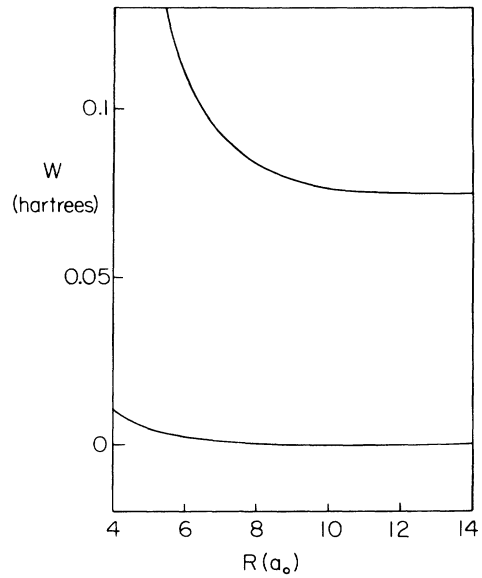

FIG. 1. The potential-energy surfaces W_1 (lower curve) and W_2 (upper curve) of model 2.

C. Na-Ar

The parameters for the Na-Ar system are chosen to correspond to the experimental conditions of Sizer and Raymer.[6] The wavelength of the laser is $\lambda = 16\,916$ cm^{-1}, which is at resonance with the $X\,^2\Sigma$–$A\,^2\Pi$ transition at $R = R_c = 9.51$. Since the transition corresponds to a weak perturbation of the dipole-allowed $3\,^2S$–$3\,^2P$ transition of atomic Na, the magnitude of the transition moment varies only slightly with respect to the internuclear distance (see, for example, Laskowski *et al.*[12]). We therefore assume $|\boldsymbol{\mu}| = \mu_0 = 2.58$. The potential-energy surface W_1 for the $X\,^2\Sigma$ state is assumed to be given by the analytic expression of Tellinghuisen *et al.*[13] and the potential-energy surface W_2 for the $A\,^2\Pi$ state by the analytic expression for $A\,^2\Pi_{1/2}$ of Goble and Winn.[14] Thus we have

$$W_1\ (\text{in cm}^{-1}) = 40.4\{1 - \exp[-0.986\,93(R - 4.994)]\}^2\{1 - 0.4988\exp[-(R - 2.5981)^2/1.2129^2]\} - 40.4 , \tag{20a}$$

$$W_2\ (\text{in cm}^{-1}) = 510.481\mu^2(1 + 0.125\,87\mu^2 - 0.0338\mu^3 + 0.035\mu^4 - 0.017\,97\mu^5 + 0.011\,75\mu^6) + 16\,961 - 572.1726 , \tag{20b}$$

$$\mu = 1 - (2.9074/R)^{4.841} , \tag{20c}$$

where the internuclear distance R appearing in Eqs. (20) should be entered in angstroms. These potential-energy surfaces W_1 and W_2 are shown in Fig. 2. In terms of the energy detuning $H_{22} - H_{11}$ and the interaction energy H_{12}, the Na-Ar system is represented by

$$H_{22} - H_{11}\ (\text{in cm}^{-1}) = W_2 - W_1 - 16\,916 , \tag{21a}$$

$$H_{12} = -\boldsymbol{\mu}_0 \cdot \mathbf{E}_0/2 , \tag{21b}$$

with W_1 and W_2 defined by Eqs. (20) and μ_0 given by 2.58. We note that the energy detuning $|H_{22} - H_{11}|$ increases even more slowly for the Na-Ar system than for model 2 as R moves away from $R_c = 9.51$. Furthermore, $|H_{22} - H_{11}|$ at large R is only 45 cm$^{-1} = 2.05 \times 10^{-4}$, to which the interaction energy $\mu_0 E_0/2$ becomes comparable at relatively low laser intensities, 10^9–10^{10} W/cm^2. For the Na-Ar system, therefore, the effect of the Rabi oscillation and the contribution from the $3\,^2S$-$3\,^2P$ transition of atomic sodium are expected to be visible even at relatively low laser intensities.

D. Comparison of the three systems

In Fig. 3 we show the energy detuning $H_{22} - H_{11}$ versus the internuclear distance R for the three systems discussed above. The energy detuning vanishes at $R_c = 9.5$ for models 1 and 2 and at $R_c = 9.51$ for Na-Ar. Model 1 shows the most rapid variation of $H_{22} - H_{11}$ with respect to R while the Na-Ar system exhibits the slowest variation.

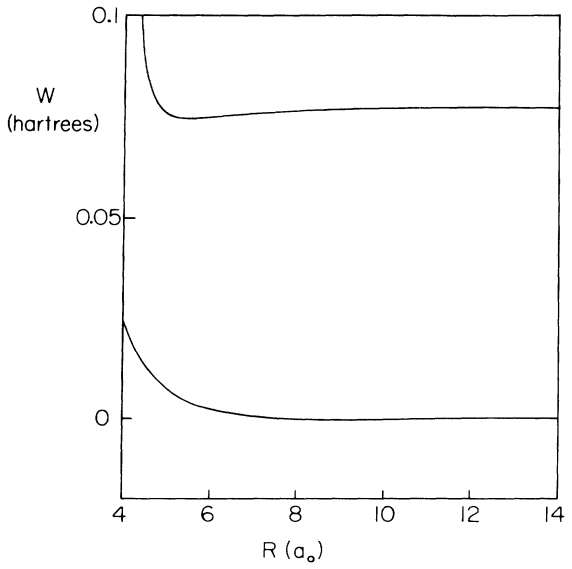

FIG. 2. The potential-energy surfaces for the $X\,^2\Sigma$ state (lower curve) and the $A\,^2\Pi$ state (upper curve) of Na-Ar.

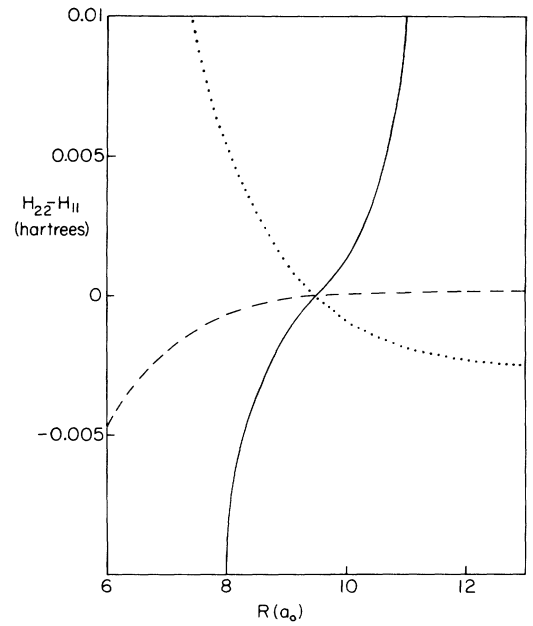

FIG. 3. The energy detuning $H_{22}-H_{11}$ vs the internuclear distance R for model 1 (solid curve), model 2 (dotted curve), and Na-Ar (dashed curve).

E. Other important system parameters

For all the three models described above, the interaction energy is determined by the scalar product of two constant vectors $\boldsymbol{\mu}_0$ and $\mathbf{E}_0$, i.e., $H_{12}=-\boldsymbol{\mu}_0\cdot\mathbf{E}_0/2$. The magnitude of the electric field amplitude $\mathbf{E}_0$, of course, is proportional to the square root of the laser intensity I. At $I=10^8$ W/cm^2, we have $E_0=|\mathbf{E}_0|=2.67\times10^{-5}$ a.u. Even if μ_0 and E_0 are given, H_{12} is different depending on the type of transition and the polarization of the laser beam. As for the polarization of the laser beam, we assume that the beam is linearly polarized in the direction of the relative velocity v of the colliding partners. The collision system then has cylindrical symmetry, which considerably simplifies the theoretical analysis. The interaction H_{12} is in turn given by

$$H_{12}=\mu_0 E_0\left[1-\left[\frac{b}{R}\right]^2\right]^{1/2}\Big/2 \tag{22a}$$

for a $\Sigma-\Sigma$ transition in which $\boldsymbol{\mu}$ is parallel to the internuclear axis, and by

$$H_{12}=\mu_0 E_0 b/2\sqrt{2}R \tag{22b}$$

for a Σ-Π transition in which $\boldsymbol{\mu}$ is perpendicular to the internuclear axis, where b is the impact parameter.

All our calculations on the short-pulse probability P_s have been made assuming that the laser pulse is a square pulse of duration $\tau=1.6$ ps (the shortest pulse used by Sizer and Raymer). Compared with this, the time interval between the two crossing points, τ_c, is taken to be 2.5 ps at $b=0$, i.e., the relative velocity v is chosen to be 1.83×10^{-4} a.u. for models 1 and 2 and 1.84×10^{-4} a.u. for the Na-Ar system. Thus, the pulse duration τ is shorter than the collision time τ_c as long as the impact parameter is smaller than $\sim0.77R_c=7.3$ a.u.

IV. RESULTS OF CALCULATIONS

In this section we present the results of our calculations carried out for each of the three systems of Sec. III using both the Landau-Zener model and the numerical Bloch approach. The probability listed is the short-pulse probability P_s calculated under the assumption that the pulse illuminates the system either on the way in or out only. We also assume that the colliding molecules are crossed perpendicularly by the laser beam, i.e., the path of the laser pulse is perpendicular to the relative velocity $\mathbf{v}$ of the colliding molecules.

A. Model 1

In Table I and Fig. 4 we show the short-pulse probability P_s calculated for model 1 using the Landau-Zener model and the numerical Bloch approach. The transition is assumed to be a Σ-Σ transition. For the numerical Bloch calculations a further assumption is made that the center of the pulse coincides with the crossing point. The probability is computed for different values of the laser intensity and two different values of the impact parameter b. As expected, the Landau-Zener model agrees well with the numerical Bloch approach for model 1, especially at low intensities. This is the result of the rapid increase in energy detuning $|H_{22}-H_{11}|$ as R moves away from R_c (see Fig. 3), restricting the transition to a narrow region around R_c. The localization of the transition within a narrow region around R_c is of course the main assumption of the Landau-Zener model. As the laser intensity is increased to $\sim10^{10}$ W/cm^2, the probability P_s climbs to ~1 and remains there until I is increased beyond $\sim10^{13}$

TABLE I. The short-pulse probability P_s for a Σ-Σ transition in model 1 calculated at different values of the pulse intensity I and impact parameter b using the Landau-Zener (LZ) model and the numerical Bloch (NB) approach.

b (a.u.)		I (W/cm^2) 10^8	5×10^8	10^9	5×10^9	10^{10}	5×10^{10}
1	LZ	0.027 01	0.1280	0.2395	0.7457	0.9353	1.0000
	NB	0.024 63	0.1175	0.2223	0.7364	0.9557	0.9714
5	LZ	0.023 14	0.1105	0.2087	0.6898	0.9038	1.0000
	NB	0.022 81	0.1089	0.2062	0.6871	0.9006	0.9885
		10^{11}	5×10^{11}	10^{12}	5×10^{12}	10^{13}	3×10^{13}
1	LZ	1.0000	1.0000	1.0000	1.0000	1.0000	1.0000
	NB	0.9999	0.9945	0.9980	0.9497	0.9351	0.8368
5	LZ	1.0000	1.0000	1.0000	1.0000	1.0000	1.0000
	NB	0.9996	0.9978	0.9926	0.9639	0.9318	0.8186

W/cm^2. It is this range of intensity (10^{10}–10^{13} W/cm^2) for which the short-pulse effect is significant, because the cw or long-pulse probability $P_{cw}=2P_s(1-P_s)$ is small when $P_s\sim1$. For model 1, therefore, the short-pulse effect can be seen over a wide range of the laser intensity.

After reaching the value of ~1, the probability P_s is expected to decrease upon further increase of the intensity as the Rabi oscillation sets in. We see indeed that the probability calculated by the numerical Bloch approach shows a decrease as the laser intensity is increased beyond $\sim10^{13}$ W/cm^2, a feature the Landau-Zener model fails to show. One notes, however, that the decrease is very slow. This can be understood if we recall that, for the model under consideration, the energy detuning $|H_{22}-H_{11}|$ varies rapidly with R. As the system moves past the crossing point R_c, the axis of the rotation of the vector **R** turns rapidly from the x axis to the z axis, effectively turning off the transition immediately after the crossing point. All in all, our data shown in Table I and Fig. 4 confirm our expectation: Model 1 represents the system for which the short-pulse effect is the strongest and the simple Landau-Zener model works well.

For further study of the probability, we show in Fig. 5 the short-pulse probability P_s at $I=2\times10^{10}$ W/cm^2 calculated using the numerical Bloch approach for different values of the impact parameter b. The probability is seen to remain relatively constant over the entire range $0\le b<R_c$, provided b is not too close to R_c. This is what one would expect for a Σ-Σ transition because the interaction energy given by Eq. (22a) at $R=R_c$ varies slowly with respect to b unless $b\approx R_c$. As b approaches R_c, the interaction energy decreases sharply, accounting for the decrease in P_s shown in Fig. 5.

We recall that the numerical Bloch probabilities shown

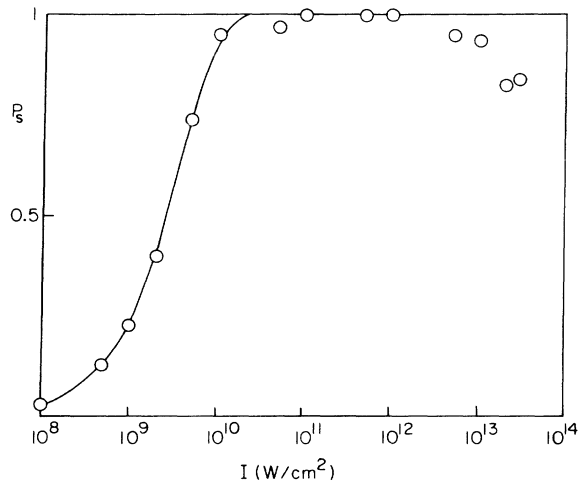

FIG. 4. The short-pulse probability P_s at impact parameter $b=1$ for a Σ-Σ transition in model 1. The solid curve represents the probability calculated by the Landau-Zener model and the circles by the numerical Bloch approach.

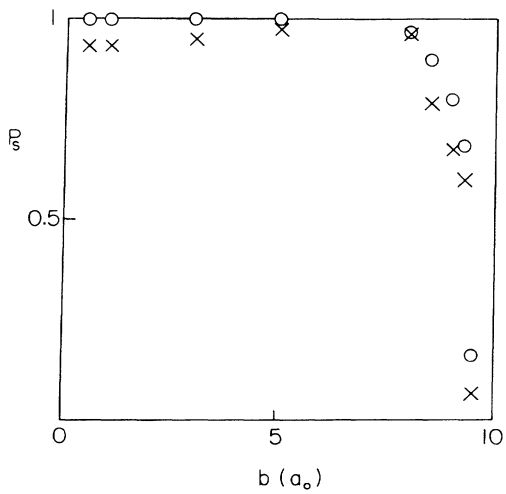

FIG. 5. The short-pulse probability P_s vs impact parameter b at $I=2\times10^{10}$ W/cm^2 for a Σ-Σ transition calculated using the numerical Bloch approach. The circles represent the probabilities for model 1 and the X's for model 2.

in Table I, and Figs. 4 and 5 are calculated assuming that the center of the pulse coincides with the crossing point. This is true only for a small fraction of the colliding pairs. In order to study the effect of the time difference t_d between the center of the pulse and the crossing point, we have calculated the probability P_s using the numerical Bloch approach at $I=2\times10^{10}$ W/cm^2 and $b=1$ for different values of t_d. The result is shown in Fig. 6 where P_s is plotted against t_d. The time difference t_d is defined in such a way that, if $t_d>0$, the center of the pulse coincides with the internuclear separation greater than $R_c=9.5$. If $|t_d|>0.8$ ps, no part of the pulse illuminates the system at the time for which $R=R_c$, and thus the Landau-Zener probability would vanish. The numerical Bloch approach presented in Fig. 6 shows the similar behavior: The probability at $t_d=\pm0.8$ ps drops to $\sim\frac{1}{2}$ of the probability at $t_d=0$. If $|t_d|$ is increased beyond 0.8 ps, the probability drops sharply.

So far the probabilities are calculated assuming that the transition is a Σ-Σ transition. We now present the result of calculations made under the assumption that the transition is a Σ-Π transition. Table II shows the short-pulse probability P_s at two different values of I and two different values of b with $t_d=0$. The Landau-Zener model and the numerical Bloch approach are seen to agree well with each other. The main difference between the types of transition arises from the difference in the interaction energy as given by Eq. (22a) for a Σ-Σ transition and by Eq. (22b) for a Σ-Π transition. In particular, the probability P_s for a Σ-Π transition is expected to increase as b is increased because of the linear dependence of H_{12} on b. This is clearly indicated in Table III where the Landau-Zener probability is large only when b is relatively large, i.e., when $b\gtrsim7$. This makes the theoretical analysis and experimental observation of the short-pulse effect very difficult, because the transition is made mainly at large values of b at which an extremely short pulse is required to separate the two crossing points. For the pulse duration of $\tau=1.6$ ps which we have chosen, the difference between the short-pulse probability and the cw or long-pulse probability becomes obscure for much of the b values over which the transition probability is significant. One therefore should probably go with a Σ-Σ transition rather than a Σ-Π transition if a clean observation of the short-pulse effect is desired.

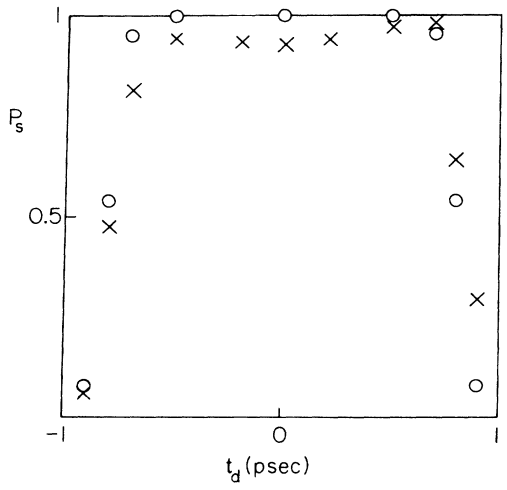

FIG. 6. The short-pulse probability P_s vs the time difference t_d between the center of the pulse and the crossing point for a Σ-Σ transition calculated at $I=2\times10^{10}$ W/cm^2 and $b=1$ using the numerical Bloch approach. The circles represent the probabilities for model 1 and the X's for model 2.

TABLE II. The short-pulse probability P_s for a Σ-Π transition in model 1 calculated using the Landau-Zener (LZ) model and the numerical Bloch (NB) approach.

b (a.u.)		I (W/cm^2) 10^8	5×10^8
1	LZ	0.000 153 4	0.000 766 8
	NB	0.000 139 7	0.000 697 2
5	LZ	0.004 475	0.022 18
	NB	0.004 353	0.021 51

B. Model 2

In Table IV and Fig. 7 we show the probability P_s calculated for model 2 assuming that the transition is a Σ-Σ transition and the center of the pulse coincides with the crossing point. As in model 1, we see generally good agreement between the Landau-Zener probabilities and the numerical Bloch probabilities at low laser intensities ($I\lesssim2\times10^{10}$ W/cm^2). However, there exists a significant difference between the two sets of the probabilities at high intensities ($I\gtrsim5\times10^{10}$ W/cm^2). This is attributed to the inability of the Landau-Zener model to properly describe the decrease in probability due to the Rabi oscillation. For model 2 the energy detuning varies more slowly than for model 1 (see Fig. 3), and thus the probability P_s decreases more rapidly after it reaches a value of ~1. In fact, the probabilities calculated by the numerical Bloch approach indicate that P_s decreases from ~1 at 1.5×10^{10} W/cm^2 to ~0.6 at 3×10^{12} W/cm^2, a fast decrease compared with the decrease in model 1. Because of this fast decrease, the range of intensity over which the probability P_s is large (~1), i.e., over which the short-pulse effect is significant, is much narrower [10^{10}—(5×10^{10}) W/cm^2] in model 2 than in model 1. As I is increased beyond $\sim5\times10^{10}$ W/cm^2, the difference between the short-pulse probability P_s and the cw or long-pulse probability P_{cw} becomes less significant.

Figures 5 and 6 show the variation of the probability P_s, calculated for model 2 using the numerical Bloch approach, with respect to b and t_d, respectively, at $I=2\times10^{10}$ W/cm^2. One can clearly see that essentially the same behavior is shown by models 1 and 2. All the discussions given in Sec. IV A for model 1 on the b and t_d dependences of P_s can equally be applied here. The behavior indicated by Figs. 5 and 6 is characteristic of a Σ-Σ transition.

A new feature that appears here but was absent in

TABLE III. The short-pulse probability P_s vs impact parameter b for a Σ-Π transition in model 1 calculated at $I=10^8$ W/cm^2 using the Landau-Zener model.

b (a.u.)	0	1	2	3	4
P_s	0	0.000 153 4	0.000 624 1	0.001 446	0.002 687
	5	6	7	8	9
	0.004 475	0.007 059	0.011 00	0.017 94	0.037 68

model 1 is the possibility of the noncollisional atomic transition. As pointed out in Sec. III, the energy detuning at large R for this model is 0.0027, and the interaction energy given by Eq. (22a) becomes comparable to it at a laser intensity of 10^{11}–10^{12} W/cm^2. At this intensity the system can be excited not only by the collisional transition but also by the atomic transition. The probability for the atomic transition for the case of a square pulse of duration τ is given by the well-known formula[9]

$$P_a = P_{\max}\sin^2\{[(\omega-\omega_a)^2+(\mu E_0/\hbar)^2]^{1/2}\tau/2\} , \quad (23a)$$

where

$$P_{\max} = \frac{(\mu E_0/2\hbar)^2}{[(\omega-\omega_a)^2+(\mu E_0/\hbar)^2]/4} \quad (23b)$$

and ω_a is the atomic frequency. In Table IV and Fig. 7 we present $P_{\max}$ for the atomic transition in model 2 as well as the Landau-Zener and numerical Bloch probabilities for the collisional transition. As expected, $P_{\max}$ becomes comparable to the probability for the collisional transition if the laser intensity exceeds $\sim 10^{11}$ W/cm^2. The observation of the short-pulse effect will therefore be difficult unless there is a way to clearly eliminate the contribution from the atomic transition.

C. Na-Ar

In Table V we show both the Landau-Zener and numerical Bloch probabilities calculated at different values of the laser intensity I and different values of the impact parameter b for the $X\,^2\Sigma$-$A\,^3\Pi$ transition of the Na-Ar system. As before, the center of the pulse is assumed to coincide with the crossing point. In Fig. 8 the Landau-Zener and numerical Bloch probabilities at $b=7$ are plotted against the intensity I. Also plotted is $P_{\max}$, given by Eq. (23b), for the $3\,^2S$-$3\,^2P$ transition of atomic sodium. We note that the probability P_s for the collisional transition is already high at a laser intensity as low as 10^9 W/cm^2, reflecting the slow increase of the energy detuning as R moves away from R_c (see Fig. 3). At the same time, the probability already begins to decrease as the intensity is increased beyond 5×10^9 W/cm^2. Thus the Landau-Zener method yields an inaccurate probability for the Na-Ar system if the laser intensity exceeds $\sim 5\times10^9$ W/cm^2. A significant feature displayed in Fig. 8 is the prominent role played by the noncollisional atomic transition: The probability for the atomic transition is comparable to the probability for the collisional transition at all laser intensities. In particular, we note that, at $I\sim10^9$ W/cm^2 at which the collisional probability becomes significant at

TABLE IV. The short-pulse probability P_s for a Σ-Σ transition in model 2 calculated at different values of the pulse intensity I and impact parameter b using the Landau-Zener (LZ) model and the numerical Bloch (NB) approach. The last row shows $P_{\max}$ for the atomic transition.

		I(W/cm^2)					
b (a.u.)		10^8	5×10^8	10^9	5×10^9	10^{10}	5×10^{10}
1	LZ	0.026 80	0.1270	0.2379	0.7429	0.9339	1.0000
	NB	0.029 45	0.1422	0.2714	0.7317	0.8774	0.9153
5	LZ	0.022 96	0.1097	0.2073	0.6870	0.9020	1.0000
	NB	0.019 18	0.091 04	0.1723	0.7057	0.9317	0.9266
				$P_{\max}$			
		0.000 856 6	0.004 268	0.008 500	0.041 10	0.078 96	0.3000
		10^{11}	5×10^{11}	10^{12}	5×10^{12}	10^{13}	3×10^{13}
1	LZ	1.0000	1.0000	1.0000	1.0000	1.0000	1.0000
	NB	0.8630	0.7254	0.6756	0.5986	0.6091	0.5418
5	LZ	1.0000	1.0000	1.0000	1.0000	1.0000	1.0000
	NB	0.8724	0.7218	0.6448	0.5788	0.6084	0.6346
				$P_{\max}$			
		0.4616	0.8108	0.8955	0.9772	0.9885	0.9961

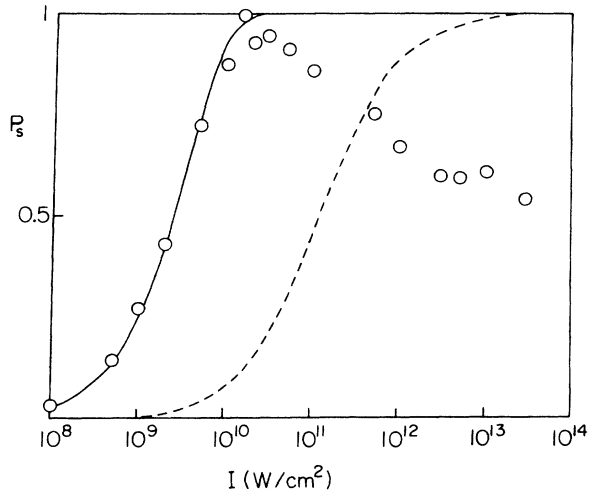

FIG. 7. The short-pulse probability P_s at impact parameter $b=1$ for a Σ-Σ transition in model 2. The solid curve represents the probability calculated by the Landau-Zener model and the circles by the numerical Bloch approach. The dashed curve is P_{max} for the atomic transition.

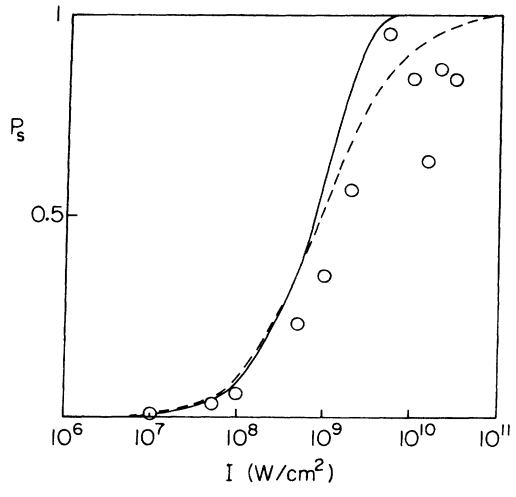

FIG. 8. The short-pulse probability P_s at impact parameter $b=7$ for the $X\,^2\Sigma$-$A\,^2\Pi$ transition of Na-Ar. The solid curve represents the probability calculated by the Landau-Zener model and the circles by the numerical Bloch approach. The dashed curve is P_{max} for the $3\,^2S$-$3\,^2P$ transition of atomic sodium.

large b, the atomic probability also becomes large. This occurs because the interaction energy becomes comparable to the asymptotic detuning of 45 cm^{-1} when the laser intensity reaches $\sim 10^9$–10^{10} W/cm^2, as noted in Sec. III. It therefore seems necessary to separate the atomic contribution from the collisional contribution if a clean observation of the short-pulse effect in Na-Ar collisions is desired. Sizer and Raymer[6] have suggested variations of Ar pressure and of laser detuning from the atomic resonance line as possible ways of separating the two contributions.

Figure 9 shows the collisional probability P_s versus the impact parameter b calculated using the numerical Bloch approach at $I=2\times 10^9$ W/cm^2. One immediately notes a rather sharp increase in probability as b is increased from 0 to the crossing point $R_c=9.51$, a trend characteristic of

TABLE V. The short-pulse probability P_s for the $X\,^2\Sigma$-$A\,^2\Pi$ transition of Na-Ar calculated at different values of the pulse intensity I and impact parameter b using the Landau-Zener (LZ) model and the numerical Bloch (NB) approach. The last row shows P_{max} for the $3\,^2S$-$3\,^2P$ transition of atomic sodium.

		I(W/cm^2)					
b (a.u.)		10^6	5×10^6	10^7	5×10^7	10^8	5×10^8
5	LZ	0.000 365 6	0.001 827	0.003 650	0.018 12	0.035 91	0.1671
	NB	0.000 280 8	0.001 407	0.002 853	0.014 25	0.028 07	0.1228
7	LZ	0.000 900 3	0.004 493	0.008 966	0.044 03	0.086 13	0.3626
	NB	0.000 723 5	0.003 394	0.006 805	0.033 16	0.063 66	0.2329
				P_{max}			
		0.001 128	0.005 612	0.011 16	0.053 42	0.1014	0.3608
				P_{max}			
		10^9	5×10^9	10^{10}	3×10^{10}		
5	LZ	0.3063	0.8393	0.9742	1.0000		
	NB	0.2105	0.6724	0.9554	0.7300		
7	LZ	0.5937	0.9889	0.9999	1.0000		
	NB	0.3514	0.9556	0.8391	0.8410		
				P_{max}			
		0.5302	0.8495	0.9186	0.9713		

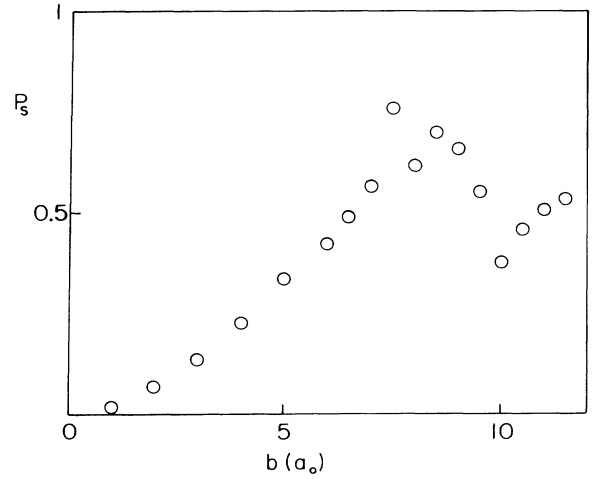

FIG. 9. The short-pulse probability P_s vs impact parameter b at $I=2\times10^9$ W/cm^2 for the $X^2\Sigma$-$A^2\Pi$ transition of Na-Ar calculated using the numerical Bloch approach.

a Σ-Π transition already noted in model 1. In fact, our calculations indicated (although not shown in Table V) that for small b the probability remains small even at $I=10^{10}$ W/cm^2, whereas for large b ($b\gtrsim5$) the probability already becomes significant at $I=5\times10^9$ W/cm^2. Since the probability is relatively large for large b's ($b=5$–9.5) at laser intensities 10^9 W/cm$^2\lesssim I\lesssim10^{10}$ W/cm^2, this range of intensity seems to offer the best chance for the observation of the short-pulse effect. The problem, however, is that for these large b values, the pulse needs to be extremely short to separate the two crossing points.

It is interesting to note that the calculations of Sizer and Raymer[6] indicate that the short-pulse effect becomes significant at a laser intensity of 10^8 W/cm^2, although their observed intensity at which the effect is significant is much higher (at least $\sim10^{10}$ W/cm^2). At this intensity, however, a significant portion of their observed fluorescence signal would originate from the $3\,^2S$-$3\,^2P$ transition of atomic sodium, according to our estimate. Sizer and Raymer, on the other hand, found no evidence of any significant contribution from the atomic transition.

V. DISCUSSION

We now summarize our findings obtained by comparing the three systems, models 1 and 2 and Na-Ar:

(1) As is well know from a simple argument based on the Landau-Zener model and confirmed by our calculations using the numerical Bloch approach, the parameter that largely determines the intensity dependence of the short-pulse probability P_s is the energy detuning $|H_{22}-H_{11}|$, in particular, the behavior of the energy detuning in the neighborhood of the crossing point R_c. If one considers a system in which $|H_{22}-H_{11}|$ increases rapidly as R moves away from R_c (as in model 1), the probability P_s increases slowly with respect to the intensity, requiring a high intensity for an observation of the short-pulse effect. Such a system, however, has an advantage in that once the probability has reached a high value, it decreases slowly upon a further increase of the intensity, giving a wide range of intensity over which the short-pulse effect can be observed.

(2) The energy detuning $|H_{22}-H_{11}|$ at asymptotic separations is also important as it determines the probability of noncollisional atomic transitions. Unless the detuning is very large, there exists a good possibility that the collisional transition occurs simultaneously with the atomic transition, especially at the high laser intensities of our interest. This is true even if the detuning of the two atomic states is large compared with the linewidth of the laser pulse. For example, the linewidth of a 1.6-ns pulse is 3.3 cm^{-1}, small compared with the energy detuning (45 cm^{-1}) of the $3\,^2S$-$3\,^2P$ atomic transition with the laser wavelength $\lambda=16\,916$ cm^{-1}. And yet the probability for the atomic transition is high if the laser intensity is $I\gtrsim10^9$ W/cm^2.

(3) The type of transition, i.e., whether it is a Σ-Σ or Σ-Π type, also has an important bearing on the short-pulse effect. Assuming that the laser beam is linearly polarized in the direction of the radiative velocity $\mathbf{v}$ of the colliding molecules, the short-pulse probability varies slowly with respect to b for the entire range of $0\lesssim b\lesssim R_c$ if the transition is a Σ-Σ transition. The pulse duration can thus remain shorter than the time between the two crossing points for a wide range of b over which the probability P_s is significant, a necessary condition for an observation of the short-pulse effect. On the other hand, the probability for a Σ-Π transition increases sharply as b is increased from 0 to R_c. The transition occurs mainly at large b's at which an extremely short pulse is required to separate the two crossing points. It therefore seems advantageous to choose a Σ-Σ transition rather than a Σ-Πtransition, but this is true for the particular polarization we have assumed. If the laser beam used is unpolarized, for example, no such difference between the two types of transition is expected to be present.

We emphasize that the theory given in this paper is by no means a complete description of the complex collision process occurring in the presence of a short laser pulse. Rather, we hope to provide a first step toward such a description. In particular, we note that the probabilities presented in this work are calculated at a given value of impact parameter b, relative velocity v, and the time difference t_d between the center of the pulse and the crossing point. Obviously, appropriate averaging must be taken in order to compare the theory with experimental data. It is expected that the averaging reduces the difference between the short-pulse probability P_s and the cw (or long-pulse) probability $P_{\rm cw}$. Another factor that should bear importance is the shape of the laser pulse. Although we assumed a square pulse, the actual laser pulse is probably better approximated by a Gaussian. Each colliding pair then experiences a continuous change in the pulse intensity and samples a different intensity at or near the crossing point, requiring another averaging over the profile of the pulse intensity. Previous calculations[6,15] indicate that the short-pulse effect is sometimes considerably weaker with a Gaussian pulse than with a square pulse.

Considering all this, it perhaps can be understood why the experimental data of Sizer and Raymer indicates that the differences between the short-pulse case and the long-pulse case show up at a higher pulse intensity than the theory predicts. The main emphasis of this paper, however, is not an analysis of their experimental data but the understanding of the kinematics and dynamics of the pulse-induced collisions at the fundamental level.

ACKNOWLEDGMENTS

This research was supported in part by the National Science Foundation under Grant Nos. CHE-8512406 and CHE-86-20274 and by the Air Force Office of Scientific Research (AFSC), United States Air Force, under Contract No. F49620-86-C-0009.

[1]T. F. George, I. H. Zimmerman, P. L. DeVries, J. M. Yuan, K. S. Lam, J. C. Bellum, H. W. Lee, M. S. Slutsky, and J. T. Lin, in *Chemical and Biochemical Applications of Lasers*, edited by C. B. Moore (Academic, New York, 1979), Vol. IV, p. 253 ff.

[2]L. I. Gudzenko and S. I. Yakovlenko, Zh. Eksp. Teor. Fiz. **62**, 1686 (1972) [Sov. Phys.—JETP **35**, 877 (1972)]; V. S. Lisitsa and S. I. Yakovlenko, *ibid.* **66**, 1550 (1974); **39**, 759 (1974)]; N. M. Kroll and K. M. Watson, Phys. Rev. A **13**, 1018 (1976); J. I. Gersten and M. H. Mittleman, J. Phys. B **9**, 383 (1976); J. M. Yuan, J. R. Laing, and T. F. George, J. Chem. Phys. **66**, 1107 (1977); S. Geltman, J. Phys. B **10**, 3057 (1977); J. Light and A. Szöke, Phys. Rev. A **18**, 1363 (1978); M. H. Nayfeh and M. G. Payne, *ibid.* **17**, 1695 (1978).

[3]R. W. Falcone, W. R. Greene, J. C. White, J. F. Young, and S. E. Harris, Phys. Rev. A **15**, 1333 (1977); A. Weingartshofer, J. K. Holmes, G. Caudle, E. M. Clarke, and H. Krüger, Phys. Rev. Lett. **39**, 269 (1977); A. V. Hellfeld, J. Caddick and J. Weiner, *ibid.* **40**, 1369 (1978); Ph. Cahuzak and P. E. Toschek, *ibid.* **40**, 1087 (1978); W. R. Green, J. Lukasik, J. R. Willison, M. D. Wright, J. F. Young, and S. E. Harris, *ibid.* **42**, 970 (1979); J. Lukasik and S. C. Wallace, *ibid.* **47**, 240 (1981); P. D. Kleiber, K. Burnett and J. Cooper, *ibid.* **47**, 1595 (1981).

[4]H. W. Lee, P. L. DeVries, and T. F. George, J. Chem. Phys. **69**, 2596 (1978); H. W. Lee, P. L. DeVries, I. H. Zimmerman, and T. F. George, Mol. Phys. **36**, 1693 (1978).

[5]H. W. Lee and T. F. George, J. Phys. Chem. **83**, 928 (1979).

[6]T. Sizer II and M. G. Raymer, Phys. Rev. Lett. **56**, 123 (1986); (unpublished).

[7]L. Landau, Phys. Z. Sowjetunion **2**, 46 (1932); C. Zener, Proc. R. Soc. London Ser. A **137**, 696 (1932).

[8]See, for example, J. C. Tully, in *Dynamics of Molecular Collisions*, edited by W. H. Miller (Plenum, New York, 1976), Part B, p. 218 ff.

[9]See, for example, L. Allen and J. H. Eberly, *Optical Resonance and Two-Level Atoms* (Wiley, New York, 1975), p. 28; M. Sargent III, M. O. Scully, and W. E. Lamb, Jr., *Laser Physics* (Addison-Wesley, MA, 1974), p. 91 ff.

[10]H. W. Lee and T. F. George, Phys. Rev. A **29**, 2509 (1984).

[11]E. C. G. Stückelberg, Helv. Phys. Acta **5**, 369 (1932).

[12]B. C. Laskowski, S. R. Langhoff, and J. R. Stallcop, J. Chem. Phys. **75**, 815 (1981).

[13]J. Tellinghuisen, A. Ragone, M. S. Kim, D. J. Auerbach, R. E. Smalley, L. Wharton, and D. H. Levy, J. Chem. Phys. **71**, 1283 (1979).

[14]J. H. Goble and J. S. Winn, J. Chem. Phys. **70**, 2051 (1979).

[15]H. W. Lee and T. F. George, in *Photons and Continuum States of Atoms and Molecules*, edited by N. K. Rahman, C. Guidotti, and M. Allegrini (Springer-Verlag, Berlin, in press).